Int. J. Heat Mass Transfer. Vol. 18, pp. 1003–1008. Pergamon Press 1975. Printed in Great Britain

DROPLET EVAPORATION: EFFECTS OF TRANSIENTS AND VARIABLE PROPERTIES*

G. L. HUBBARD, V. E. DENNY and A. F. MILLS
University of California, Los Angeles, CA 90024, U.S.A.

(*Received* 23 *July* 1974)

Abstract—A numerical study of the effects of transients and variable properties on single droplet evaporation into an infinite stagnant gas is presented. Sample calculations are reported for octane droplets, initially at 300°K with $R_0 = 0{\cdot}1$, $0{\cdot}5$, $2{\cdot}5 \times 10^{-4}$ m, evaporating into air at temperatures and pressures in the ranges 600–2000°K and 1–10 atm, respectively. It is found that initial size R_0 is eliminated from the problem on scaling time with respect to R_0^2 and that the evaporative process becomes quasi-steady with $(R/R_0)^2 = (R_0^*/R_0)^2 - \beta t/R_0^2$, as suggested by experiment. Comparisons of solutions using various reference property schemes with those for variable properties show that best agreement obtains using a simple 1/3 rule wherein properties are evaluated at $T_r = T_s + (T_e - T_s)/3$ and $m_{1,r} = m_{1,s} + (m_{1,e} - m_{1,s})/3$. The effects of temporal storage of mass species, energy, etc. and radial pressure variations in the vapor phase prove to be negligible, the early transient behavior being solely due to sensible heat effects within the droplet and related variations in vapor-side driving forces.

NOMENCLATURE

$\mathscr{B}$, vapor-side driving force;
C_p, specific heat [J/kg °K];
$\mathscr{D}_{12}$, binary diffusion coefficient [m²/s];
$\hat{h}_{fg}$, latent heat [J/kg];
k, thermal conductivity [w/m °K];
m, mass fraction;
$\dot{m}''$, mass flux [kg/m² s];
M, molecular weight;
P, pressure [atm, N/m²; 1 atm = $1{\cdot}013 \times 10^5$ N/m²];
Pr, Prandtl number;
r, radial coordinate [m];
R, droplet radius [m];
R_0^*, intercept at $t = 0$ for quasi-steady curve;
$\mathscr{R}$, universal gas constant [atm m³/kg-mole °K];
Sc, Schmidt number;
t, time [s];
T, temperature [°K];
v, radial velocity [m/s].

Greek symbols

α, thermal diffusivity [m²/s];
β, negative of slope for $(R/R_0)^2$ vs t/R_0^2 [m²/s];
Δ, measure of difference in radii or specific heats;
μ, viscosity [Ns/m²];
ρ, density [kg/m³].

Subscripts

0, at $t = 0$;
1, of evaporating species;
2, of air;
e, $r \to \infty$;
h, for heat transfer;
i, ith node point;
l, of liquid;
m, for mass transfer;
r, in the radial direction; also, at reference conditions;
s, at $r = R+$;
u, at $r = R-$.

Superscripts

0, at the previous iterate;
+, dimensionless.

INTRODUCTION

DROPLET evaporation is of importance in, for example, process operations, liquid hydrocarbon combustion, and meteorology. Evaporation of a single isolated liquid droplet into an infinite stagnant gas has long been a subject of study; recent reviews of this activity have been given by Kent [1] and Williams [2]. Engineering calculations are usually based on results of constant property quasi-steady theory which show that the droplet diameter squared decreases linearly with time, a result confirmed by experiment for all but the initial stages of droplet life. Two aspects of this theory which have received considerable attention are (i) validity of the quasi-steady assumption and (ii) accounting for variable transport properties in predicting the proportionality constant β in $(R/R_0)^2 = (R_0^*/R_0)^2 - \beta t/R_0^2$. However, neither aspect has as yet been satisfactorily resolved.

The most complete study of the transient problem was that of Kotake and Okazaki [3], who numerically integrated the governing time dependent conservation equations. Their results are often quoted when the quasi-steady assumption is evaluated, e.g. [2, 4], and although serious discrepancies with experiment have been noted, no one has suggested the possibility that the Kotake and Okazaki numerical solution procedures were in error. Examples of the discrepancies

*Computer time for the numerical calculations was supplied by the Campus Computing Network of the University of California, Los Angeles.

with experiment are: (1) plots of R^2 vs t do not show the quasi-steady constant β regime, but rather a continuous and marked decrease in β, and (2) the accompanying solutions of the related droplet combustion problem predict flame temperatures much lower than measured values. New numerical solutions of the transient problem are required to evaluate the work of Kotake and Okazaki.

Early attempts to account for variable transport properties in the prediction of β were based on ad hoc assumptions and comparisons with experiment; many such attempts were also made for the related droplet combustion problem. Recently, Kent [1] carried out extensive calculations for quasi-steady evaporation with variable properties. A limited attempt was made to determine a simple reference state for evaluation of properties in the corresponding constant property solution; however, Kent chose to correlate his results to high accuracy with specialized complex algebraic formulae. Thus, there is definite merit in ascertaining whether simpler, or more general, reference state schemes, e.g. as proposed by Knuth [5], are of adequate accuracy for the engineering calculation of droplet evaporation rates.

In the present study we have numerically integrated the mass, species and energy conservation equations governing droplet evaporation, both for variable properties and for properties using various reference state schemes. We shall show that the results reported by Kotake and Okazaki are erroneous and must be discounted. We will also make recommendations concerning a suitable reference state for use in transient and quasi-steady constant property solutions.

ANALYSIS

Governing equations

A spherical droplet of pure liquid, initially at temtemperature T_0 and radius R_0, is suddenly subjected to surrounding gas at uniform temperature T_e. The only convective motion considered is that induced by the evaporation process itself, giving rise to a radial convective velocity in the vapor (species 1) and gas (species 2) mixture. The governing conservation equations are:

1. Liquid phase, $r < R(t)$
   (A) Energy

$$\frac{\partial T}{\partial t} = \alpha_l \frac{1}{r^2}\frac{\partial}{\partial r}\left(r^2 \frac{\partial T}{\partial r}\right). \tag{1}$$

2. Vapor phase, $r > R(t)$
   (A) Mass

$$\frac{\partial \rho}{\partial t} + \frac{1}{r^2}\frac{\partial}{\partial r}(\rho r^2 v_r) = 0. \tag{2}$$

   (B) Momentum

$$\frac{\partial v_r}{\partial t} + v_r \frac{\partial v_r}{\partial r} = \frac{1}{\rho r^2}\frac{\partial}{\partial r}\left(\frac{4}{3}\mu r^2 \frac{\partial v_r}{\partial r}\right) - \frac{8}{3}\frac{\mu}{\rho}\frac{v_r}{r^2} - \frac{4}{3\rho r}\frac{v_r}{r}\frac{\partial \mu}{\partial r} - \frac{1}{\rho}\frac{\partial P}{\partial r}. \tag{3}$$

   (C) Species,

$$\frac{\partial m_1}{\partial t} + v_r \frac{\partial m_1}{\partial r} = \frac{1}{\rho r^2}\frac{\partial}{\partial r}\left(\frac{\mu}{Sc} r^2 \frac{\partial m_1}{\partial r}\right). \tag{4}$$

   (D) Energy,

$$\frac{\partial T}{\partial t} + v_r \frac{\partial T}{\partial r} = \frac{1}{\rho r^2}\frac{\partial}{\partial r}\left(\frac{\mu}{Pr} r^2 \frac{\partial T}{\partial r}\right) + \frac{\mathscr{D}_{12}}{C_p}\frac{\partial T}{\partial r} \times \left[(C_{p1} - C_{p2})\frac{\partial m_1}{\partial r} + \frac{Sc}{Pr}\frac{\partial C_p}{\partial r}\right]. \tag{5}$$

The boundary conditions and constants are:

1. Liquid phase, at $r = 0$

$$\frac{\partial T}{\partial r} = 0. \tag{6}$$

2. Vapor phase, as $r \to \infty$

$$m_1 \to 0; \quad T \to T_e; \quad v_r \to 0; \quad P \to P_e. \tag{7}$$

3. At the interface, $r = R$,

$$v_r = \dot{m}''\left(\frac{1}{\rho} - \frac{1}{\rho_l}\right) \tag{8}$$

$$(1 - m_{1,s})\dot{m}'' = -\rho \mathscr{D}_{12}\left.\frac{\partial m_1}{\partial r}\right|_s \tag{9}$$

$$T_s = T_u \tag{10}$$

$$k\left.\frac{\partial T}{\partial r}\right|_s = k\left.\frac{\partial T}{\partial r}\right|_u + \dot{m}''\hat{h}_{fg} \tag{11}$$

$$\frac{\mathrm{d}R}{\mathrm{d}t} = -\frac{\dot{m}''}{\rho_l} \tag{12}$$

$$m_{1,s} = m_{1,s}(P, T_s). \tag{13}$$

In addition, there is an equation of state; assuming ideal gas mixtures, $P = \rho \mathscr{R} T/M$. Initial conditions for the problem are, in a practical sense, somewhat arbitrary. The approach adopted here is discussed below along with other numerical procedures. Additional assumptions include (i) constant liquid phase properties, (ii) no second order diffusion effects, and (iii) thermodynamic equilibrium at the interface. Furthermore, the variable property calculations showed that P deviated from P_e by less than 0·3 per cent; thus, $P = P_e$ was assumed for the reference property analysis, making equation (3) irrelevant.

Numerical solution procedure

To effect an efficient solution algorithm for the problem, the spatial coordinate was first rescaled as follows

$$r^* = (e^{\gamma r/R} - 1)/(e^{\gamma} - 1) = (\eta - 1)/\Gamma, \quad r \leqslant R(t)$$

$$r^{**} = 1 - e^{-\delta(r-R)/R} = 1 - e^{-\delta^*(r-R)}, \quad r \geqslant R(t)$$

giving

$$\frac{\partial T}{\partial t} + \frac{f_1}{R\Gamma}\frac{\dot{m}''}{\rho_l}\frac{\partial T}{\partial r^*} = \frac{\gamma^2 \alpha_l}{R^2\Gamma^2} f_2 \frac{\partial}{\partial r^*}\left(f_3 \frac{\partial T}{\partial r^*}\right) \tag{14}$$

for $r^* \leqslant 1$ and

$$\frac{\partial \phi_n}{\partial t} + \delta^* F_1\left(v_r + F_2\frac{\dot{m}''}{\rho_l}\right)\frac{\partial \phi_n}{\partial r^{**}} = \frac{\delta^{*2} F_1}{\rho F_2^2}\frac{\partial}{\partial r^{**}}\left(\mu F_1 F_2^2 \Gamma_{\phi_n}\frac{\partial \phi_n}{\partial r^{**}}\right) + S_{\phi_n} \tag{15)–(18}$$

for $r^{**} \geqslant 0$, where $f_1 = \eta \ln \eta, f_2 = \eta/(\ln \eta)^2, f_3 = \eta(\ln \eta)^2$, $F_1 = 1 - r^{**}$, $F_2 = 1 - \delta^{-1} \ln F_1$, and for $\phi_n = T$, m_1, ρ, and v_r, respectively,

Γ_{ϕ_n}	S_{ϕ_n}
Pr^{-1}	$(\delta^{*2} F_1^2 \mathscr{D}_{12}/C_p)(\partial T/\partial r^{**})(\Delta C_p \partial m_1/\partial r^{**} + ScPr^{-1} \partial C_p/\partial r^{**})$
Sc^{-1}	0
0	$-(\delta^* F_1 \rho/F_2^2)\partial(F_2^2 v_r)/\partial r^{**}$
4/3	$-(8\mu v_r/3\rho F_2^2 R^2) - (\delta^* F_1/\rho)[(4v_r/3F_2 R)\partial\mu/\partial r^{**} + \partial P/\partial r^{**}]$.

Equations (14)–(16) were then approximated numerically, using three-point central difference expressions for spatial derivatives and backward difference expressions for temporal derivatives. In advancing the numerical solution from one time-step to the next, iteration was required to enforce strict conservation of mass and energy across the vapor–liquid interface. An iterative scheme was devised for which strong coupling between $\dot{m}''$, $m_{1,s}(T)$, and T_s at the interface was treated by linearizing equations (9) and (13) about previous iterates

$$\dot{m}'' = \dot{m}''^0 \frac{m_{1,s} - m_{1,s}^0}{1 - m_{1,s}^0} - \left.\frac{\rho \mathscr{D}_{12} \delta^*}{(1 - m_1^0)} \frac{\partial m_1}{\partial r^{**}}\right|_s \quad (19)$$

$$m_{1,s} = m_{1,s}^0 + \frac{C_1}{(T_s^0)^2} m_{1,s}^0 \left(1 - \frac{M_1 - M_2}{M_1} m_{1,s}^0\right) \times (T_s - T_s^0), \quad (20)$$

where $m_{1,s}^0$ is extracted from equation (13) in terms of the previous iterate T_s^0, and advancing the spatial distributions for T and m_1

$$T_i = A_i T_{i+1} + B_i T_{i-1} + C_i; \quad i = 1, 2, \ldots M (i \neq N) \quad (21)$$

$$m_{1,i} = D_i m_{1,i+1} + E_i m_{1,i-1} + F_i; \quad i = N+1, \ldots M \quad (22)$$

together with algebraic representations of equations (11), (14)–(16), and (19)–(20) at the interface

$$T_N = aT_{N+1} + bT_{N-1} + cm_{1,N} + dm_{1,N+1} + e \quad (23)$$

$$m_{1,N} = fT_N + g \quad (24)$$

simultaneously by means of successive substitution:

$$T_i = A_i^* T_{i+1} + B_i^* m_{1,i+1} + C_i^*$$

$$m_{1,i} = D_i^* m_{1,i+1} + E_i^* T_{i+1} + C_i^*, \quad 1 = M, M-1, \ldots N$$

$$T_i = A_i^* T_{i+1} + C_i^*, \quad i = N-1, N-2, \ldots 1.$$

With T_i and $m_{1,i}$ known, the associated ρ_i distribution was calculated, and the $v_{r,i}$ distribution extracted from equation (17) by trapezoidal integration, applying equation (8) to obtain $v_{r,N}$.

The above iterative procedure was continued until $|1 - \dot{m}''^0/\dot{m}''| \leqslant 10^{-4}$. Then, equation (18) was integrated from $r^{**} = 1$ to $r^{**} = 0$ to extract the P_i's, and the variable thermophysical properties, droplet radius, and S_{ϕ_1} for the energy equation were updated.

In all cases, the initial conditions were treated by constructing reasonable polynomial distributions for temperature and mass species, assigning $T_{r^*=0} = 300°\text{K}$, $T_s = 320°\text{K}$, and self-consistent fluxes at the vapor–liquid interface. From selected numerical experiments in which isothermal liquid-side temperature distributions were assigned as $T(r^*) = 300°\text{K}$ vs 320°K, it is concluded that the initial conditions affect the results reported below by at most 3 per cent. For a typical case coded in FORTRAN-H for the IBM 360/91 computer, ~30 s of CPU time were required with $\Delta r^* \equiv \Delta r^{**} = 0{\cdot}0125$ and $\Delta t = t|_{0{\cdot}45R_0}/300$. Based on selected trials at various Δr^*, Δr^{**}, and Δt, the numerical solutions are judged to be in error by no more than 2 per cent.

Thermophysical properties

Liquid phase properties of *n*-octane were obtained from various sources with ρ_l taken as 703·6 kg/m^3, $C_{pl} = 2420$ J/kg deg, and $k_l = 0{\cdot}116$ W/m deg. For the gas phase properties, molecular weights of 114·23 and 29·87 were used for *n*-octane and air, respectively. *n*-Octane vapor pressure was calculated from $P_{sat} = \exp(-4140°\text{K/T} + 10{\cdot}3864)$ atm., and the heat of vaporization from $h_{fg} = 2{\cdot}977 \times 10^5 - 2{\cdot}6913 \times 10^3 \zeta - 5{\cdot}5287 \times 10^3 \zeta^2 - 858{\cdot}3\zeta^3$ J/kg, where $\zeta = \ln P_{sat}$. Pure species gas phase transport properties were calculated from the Chapman–Enskog kinetic theory of gases with Lennard–Jones collision parameters of $\sigma_1 = 7{\cdot}407$ Å, $\varepsilon_1/k = 333°\text{K}$ for octane, and $\sigma_2 = 3{\cdot}617$ Å, $\varepsilon_2/k = 97°\text{K}$ for air. The Mason and Monchik mixture rule was used for viscosity [6] and the Wilke rule for thermal conductivity [7]. Species heat capacities were obtained from [8], and mixture thermodynamic properties calculated assuming an ideal gas mixture.

Reference states

The prescriptions for the various reference state schemes used to evaluate properties in the reference property solutions are as follows. In each case the values of the properties are updated at each time-step of the solution. We note that these are not *constant* property solutions inasmuch as $\partial\rho/\partial t \neq 0$.

(A) *Knuth* [5]. This scheme, as it applies to the droplet evaporation problem, is based on an approximate solution of the variable property stagnant film model assuming constant energy and mass exchange coefficients (k/C_p and $\rho\mathscr{D}_{12}$ respectively).

$$T_r = \frac{T_s - T_e}{2} - \frac{1}{12}\left(\mathscr{B}_{hr} \frac{C_{p1}}{C_{pr}} + \mathscr{B}_{mr} \frac{C_{p1} - C_{pr}}{C_{pr}}\right)(T_e - T_s)$$

$$m_{2r} = \frac{M_2}{M_2 - M_1} \frac{\ln(M_2/M_s)}{\ln(M_2/m_{2,s}M_s)}$$

$$\mathscr{B}_{hr} = \frac{\dot{m}''}{k_r/RC_{pr}}; \quad \mathscr{B}_{mr} = \frac{\dot{m}''}{1/R\rho_r \mathscr{D}_{12r}}.$$

(B) *A 1/3 rule.* It is well established for convective heat transfer, e.g. Sparrow and Gregg [9], that superior correlations are obtained when the reference temperature is evaluated closer to the wall than the mean

film value. Extending this concept to the simultaneous heat- and mass-transfer problem under consideration here,

$$T_r = T_s + 1/3(T_e - T_s)$$
$$m_{1r} = m_{1,s} + 1/3(m_{1,e} - m_{1,s}) = 2/3m_{1,s}.$$

(C) *Law and Williams* [10]. This is an empirical scheme developed to give good agreement with alkane droplet burning rates and quasi-steady theory.

$$T_r = T_s + 0{\cdot}5(T_e - T_s)$$
$$k_r = 0{\cdot}4k_1(T_r) + 0{\cdot}6k_2(T_r)$$
$$C_{pr} = C_{p1}(T_r); \quad \mathscr{D}_{12r} = \mathscr{D}_{12}(T_r); \quad \rho_r = \frac{k_r}{C_{pr}\mathscr{D}_{12r}}.$$

RESULTS AND DISCUSSION

Table 1 lists the cases calculated together with the times required for evaporation to $0{\cdot}45R_0$ (about 90 per cent by mass evaporated). Figure 1 shows the normalized drop radius squared as a function of time scaled with the initial radius squared for the exact variable property calculations. This time-scaling successfully eliminates the dependence on initial radius; for, Cases 3, 4 and 5 lie on a single curve. Clearly demonstrated is the characteristic monotonic increase in β, the negative of the slope of these curves, as has been found in numerous experiments. The initial low values prevail while the droplet is absorbing sensible heat; while, the quasi-steady asymptotic value obtains when the droplet is isothermal at the wet-bulb temperature. To confirm that the unsteady behavior is due essentially to the liquid phase temperature transient, selected calculations were made wherein the gas phase time derivatives were deleted; in no case were deviations in $\dot{m}''$ greater than 1 per cent. Figure 1 also shows that the cases chosen for study cover a wide range of quasi-steady β values.

Figure 2 is reproduced from Kotake and Okazaki [3] and gives the results of their calculations for methyl-alcohol droplets of initial radius 0·001 m. These authors also obtained results for *n*-octane but present data only for $T_e = 300°C$; however, that data is qualitatively very similar to the data in Fig. 2. The full lines are for their unsteady calculations; while, the dashed lines are solutions assuming a quasi-steady gas phase. It can be seen that the unsteady results bear no resemblance to those obtained in the present study, and also no resemblance to their own quasi-steady gas phase results. We conclude that the numerical solution procedure used by Kotake and Okazaki was in error, and suggest that their results be discarded.

Figure 3 shows temperature profiles for Case 3. The time required for R to decrease to $0{\cdot}45R_0$ was $6{\cdot}60 \times 10^{-4}$ s, so the profiles depicted span most of the droplet life. An interesting feature of these graphs is the "blowing" effect seen in the gas phase. To first order, the vapor-side heat-transfer conductance varies

Table 1. Parameter values for cases calculated, and times for evaporation to $0{\cdot}45R_0$

	Conditions			Time for evaporation to $0{\cdot}45R_0$ (s)			
Case	T_e (°K)	$R_0 \times 10^4$ (m)	P_e (atm)	Variable properties	Knuth [5]	1/3 rule	Law and Williams [10]
1	600	2·5	1	1·51	1·53	1·58	1·64
2	1200	2·5	1	$6{\cdot}37 \times 10^{-1}$	6·78	6·40	6·33
3	2000	0·1	1	$6{\cdot}60 \times 10^{-4}$	7·48	6·20	5·96
4	2000	0·5	1	$1{\cdot}65 \times 10^{-2}$	1·87	1·55	1·49
5	2000	2·5	1	$4{\cdot}12 \times 10^{-1}$	4·67	3·87	3·73
6	600	2·5	5	1·78	1·74	1·80	1·93
7	600	2·5	10	1·95	1·89	1·95	2·12
8	2000	0·1	10	$6{\cdot}76 \times 10^{-4}$	7·08	6·06	6·18
9	2000	2·5	10	$4{\cdot}22 \times 10^{-1}$	4·42	3·78	3·86
10	1200	2·5	10	$6{\cdot}80 \times 10^{-1}$	6·28	6·50	6·80

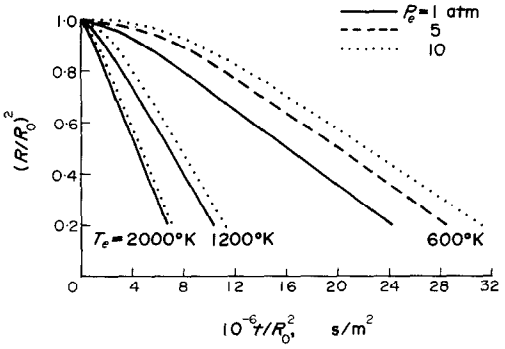

FIG. 1. Transient response of droplet radius-squared: $R_0 = 2{\cdot}5 \times 10^{-4}$ m. (At $T_e = 2000°K$, $R_0 = 0{\cdot}1$, $0{\cdot}5$, $2{\cdot}5 \times 10^{-4}$ m for $P_e = 1$ atm and $R_0 = 0{\cdot}1$, $2{\cdot}5 \times 10^{-4}$ m for $P_e = 10$ atm.)

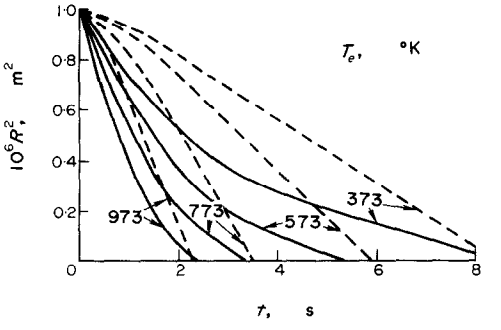

FIG. 2. Transient response of a methyl alcohol droplet—after reference [3].

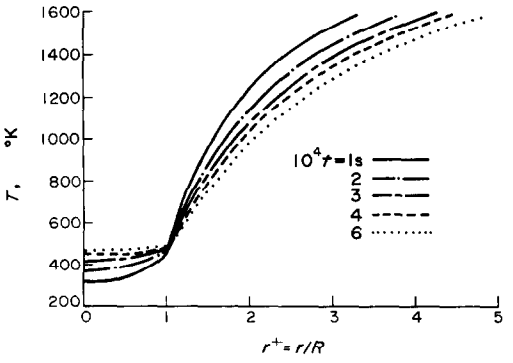

FIG. 3. Transient temperature distributions: $T_e = 2000°K$, $P_e = 10$ atm, $R_0 = 0{\cdot}1 \times 10^{-4}$ m.

inversely with $R(t)$; furthermore, as the liquid approaches the wet-bulb temperature, the rate of conduction into the droplet $(-k_l \partial T/\partial r^+|_u)$ decreases. Thus, the evaporative flux increases according to the surface energy balance, equation (11), from 3·53 kg/m²s at 1×10^{-4} s to 8·73 kg/m²s at 6×10^{-4} s. The resulting increase in $v_{r,s} = \dot{m}''/\rho_s$ reduces the temperature gradient $\partial T/\partial r^+|_s$, as clearly observed. Figure 4 shows normalized gas phase mass fractions $m_1/m_{1,s}$, also for Case 3. Again the effect of blowing in reducing the gradient $\partial m_1/\partial r^+|_s$ is clearly in evidence.

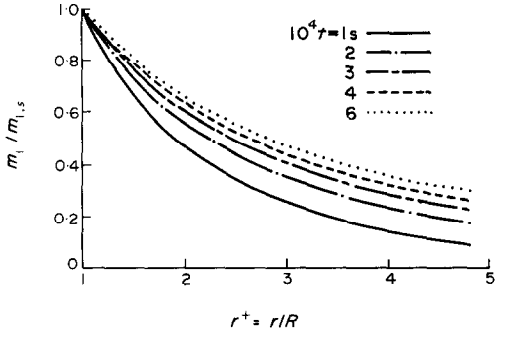

FIG. 4. Transient mass species distributions: $T_e = 2000°K$, $P_e = 10$ atm, $R_0 = 0{\cdot}1 \times 10^{-4}$ m.

We now turn to the results of our investigation of reference states for the evaluation of properties. We note first that the mean square deviations of the evaporation times for the ten cases reported in Table 1 are (a) Knuth: 9·25 per cent, (b) 1/3 rule: 6·28 per cent, and (c) Law and Williams: 8·58 per cent. The evaporation times reported in Table 1 are related to integral averages of evaporation rate over 90 per cent of the droplet life. Added insight is obtained from Figs. 5 and 6, where a dimensional evaporation rate is plotted as a function of time for Cases 1 and 3 respectively. It is seen that the deviations of the reference property solutions are greatest in the central period of droplet life where the evaporation rates are highest.

A number of other reference schemes were investigated but were less successful than those reported in detail here. For example, in scheme B the 1/3 factor

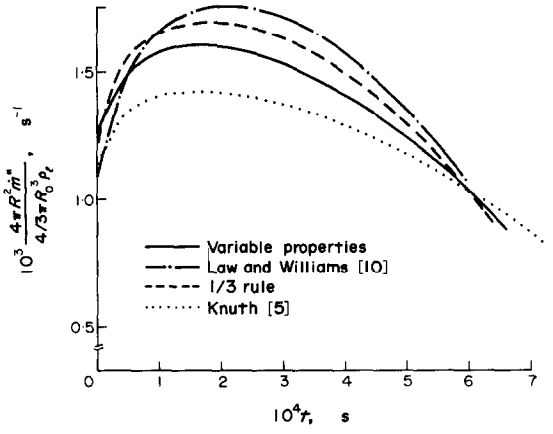

FIG. 5. Comparisons of reference property schemes with exact solutions: $T_e = 2000°K$, $P_e = 1$ atm, $R_0 = 0{\cdot}1 \times 10^{-4}$ m.

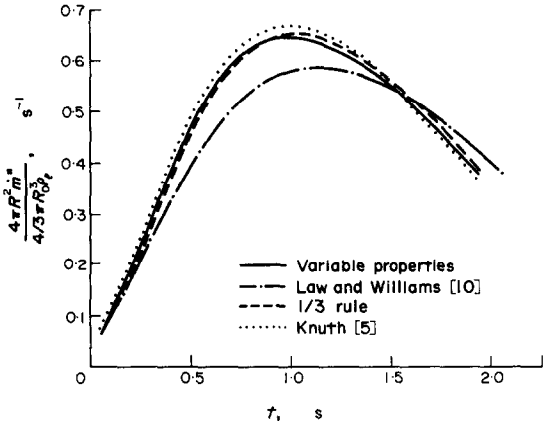

FIG. 6. Comparisons of reference property schemes with exact solutions: $T_e = 600°K$, $P_e = 1$ atm, $R_0 = 2{\cdot}5 \times 10^{-4}$ m.

was replaced by 1/2; i.e. the mean film values of temperature and concentration, but the results were inferior. Also $T_r = T_s + 1/3(T_e - T_s)$ was used in the Law and Williams scheme with inferior results. In an attempt to obtain a really simple scheme pure air properties were used at various temperatures; with $T_r = T_s$ this scheme worked surprisingly well, but was generally inferior to the three schemes reported here. Finally, check calculations were performed assuming a well-stirred model for the liquid phase (by letting $k_l \to \infty$); no substantive changes to the observations made above were noted. Thus, we recommend Scheme B, the 1/3 rule, for general use.

CONCLUSIONS

1. The transient evaporation of single droplets into an infinite stagnant gas is independent of initial size provided time is scaled with respect to the initial radius-squared.

2. The evaporative process becomes quasi-steady, with $(R/R_0)^2 = (R_0^*/R_0)^2 - \beta t/R_0^2$, as suggested by experiment; thus, the results of Kotake and Okazaki are presumed erroneous and should be discarded.

3. As quasi-steady evaporation is approached, the effects of blowing in reducing the normalized temperature and species gradients in the vapor at the droplet surface are enhanced.

4. For purposes of engineering calculations, the most appropriate reference state for evaluation of properties is a simple 1/3 rule wherein the reference temperature and species mass fraction are, respectively

$$T_r = T_s + 1/3(T_e - T_s)$$
$$m_{1,r} = m_{1,s} + 1/3(m_{1,e} - m_{1,s}).$$

REFERENCES

1. J. C. Kent, Quasi-steady diffusion-controlled droplet evaporation and condensation, *Appl. Scient. Res., Ser.* **A28**, 315–359 (1973).
2. A. Williams, Combustion of droplets of liquid fuels: a review, *Combust. Flame* **21**, 1–31 (1973).
3. S. Kotake and T. Okazaki, Evaporation and combustion of fuel droplet, *Int. J. Heat Mass Transfer* **12**, 595–610 (1969).
4. F. R. Newbold and N. R. Amundson, A model for evaporation of a multi-component droplet, *A.I.Ch.E. Jl* **19**, 22–30 (1973).
5. E. L. Knuth, Use of reference states and constant property solutions in predicting mass-, momentum- and energy-transfer rates in high-speed laminar flows, *Int. J. Heat Mass Transfer* **6**, 1–22 (1963).
6. E. A. Mason and L. Monchik, Transport properties of polar gas mixtures, *J. Chem. Phys.* **36**, 2746–2757 (1962).
7. D. K. Edwards, V. E. Denny and A. F. Mills, *Transfer Processes*, p. 210. Holt, Rinehart and Winston, New York (1973).
8. *Nonmetallic Elements, Compounds and Mixtures*, P.R.C. Data Book, Vol. 2, Purdue Research Foundation (1966).
9. E. M. Sparrow and J. L. Gregg, The variable fluid-property problem in free convection, *Trans. Am. Soc. Mech. Engrs* **80**, 879–886 (1958).
10. C. K. Law and F. A. Williams, Kinetics and convection in the combustion of alkane droplets, *Combust. Flame* **19**, 393–405 (1972).

EVAPORATION D'UNE GOUTTELETTE: EFFETS DE LA PERIODE TRANSITOIRE ET DES PROPRIETES VARIABLES

Résumé—On présente une étude numérique des effets de la période transitoire et des propriétés variables sur l'évaporation d'une gouttelette unique dans un gaz infini au repos. Des exemples de calculs sont présentés pour des gouttelettes d'octane initialement à 300 K avec $R_0 = 0{,}1$–$0{,}5$–$2{,}5 . 10^{-4}$ m s'évaporant dans l'air à des températures et des pressions respectivement dans les domaines 600–2000 K et 1–10 atm. On trouve que la dimension initiale R_0 n'intervient plus dans le problème lorsque l'échelle de temps est rapportée à R_0^2 et que le processus d'évaporation devient quasi-stationnaire lorsque $(RR_0)^2 = (R_0^* R_0)^2 - \beta t R_0^2$, comme le suggère l'expérience. Les comparaisons des solutions utilisant des combinaisons variées de propriétés de référence avec celles à propriétés variables montrent que le meilleur accord s'obtient en utilisant une loi simple 1,3 dans laquelle les propriétés sont évaluées à $T_r = T_s + (T_e - T_s)^3$ et $m_{i,r} = m_{i,s} + (m_{i,e} - m_{i,s})^3$. Les effets de mise en mémoire temporaire des espèces massiques, de l'énergie, etc. et des variations radiales de pression dans la phase vapeur se sont avérés négligeables, la première évolution transitoire étant seulement dûe aux effets de chauffage sensibles dans la gouttelette et aux variations qui s'y rattachent des forces actives du côté vapeur.

TROPFENVERDAMPFUNG: DER EINFLUSS VON INSTATIONÄREN UND VERÄNDERLICHEN STOFFEIGENSCHAFTEN

Zusammenfassung—Es wird eine rechnerische Untersuchung der Einflüsse von instationären und veränderlichen Stoffeigenschaften auf die Verdampfung eines einzelnen Tropfens in ein unbegrenztes ruhendes Gas vorgelegt. Es wird ein Beispiel gerechnet für Oktan-Tropfen, die bei einer Anfangstemperatur von 300 K mit $R_0 = 0{,}1$; 0,5; $2{,}5 \times 10^{-4}$ m in Luft verdampfen, die im Temperatur- und Druckbereich von 600 und 2000 K sowie 1 bzw. 10 atm vorliegt. Es wurde festgestellt, daß der Anfangsdurchmesser R_0 eliminiert wird durch den Zeitmaßstab unter Berücksichtigung von R_0^2 und daß, wie das Experiment zeigt, der Verdampfungsprozeß quasistationär wird mit

$$(RR_0^2) = (R_0^* R_0)^2 - \beta t R_0^2.$$

Der Vergleich einer Lösung, die sich bei verschiedenen Bezugsstoffeigenschaften ergeben hat, mit einer, die für veränderliche Stoffeigenschaften erhalten wurde, zeigt, daß sich die beste Übereinstimmung ergibt, wenn eine einfache 1/3 verwendet wird, wobei die Stoffeigenschaften bei der Temperatur $T_r = T_s + (T_e - T_s)/3$ und dem Massenanteil $m_{1,r} = m_{1,s} + (m_{1,e} - m_{1,s})/3$ berechnet werden. Des Einfluß der zeitlichen Speicherung von Massengrößen. Energie usw. sowie von radialen Druckschwankungen in der Dampfphase erweist sich als vernachlässigbar. Das anfänglich instationäre Verhalten beruht allein auf dem Einfluß der fühlbaren Wärme im Tropfen und damit verknüpften Veränderungen in den treibenden Kräften der Dampfseite.

ИСПАРЕНИЕ КАПЕЛЬ. ВЛИЯНИЕ ПЕРЕХОДНЫХ ПРОЦЕССОВ И ПЕРЕМЕННЫХ СВОЙСТВ

Аннотация — Представлено исследование (численным методом) влияния переходных процессов и переменных свойств на испарение единичной капли в бесконечный неподвижный газ. Даны примеры расчета для капель октана с начальной температурой в 300°К и R_0 равным 0,1; 0,5; $2{,}5 \times 10^{-1}$ μ, которые испарялись в воздух при температуре от 600 до 2000°К и давлении от 1 до 10 атм. Найдено, что начальный размер можно рассчитать из задачи о времени испарения. При $(R/R_0)^2 = (R_0^*/R_0)^2 - \beta t/R_0^2$, как подсказывает эксперимент, процесс испарения становится квазистационарным. Сравнение решений, в которых используются различные исходные свойства, с решениями с переменными свойствами показывает, что наилучшее согласие достигается при $T_r = T_s + (T_e - T_s)/3$ и $m_{1,r} = m_{1s} + (m_{1,e} - m_{1,s})/3$.

Влияние временного накопления массы, энергии и т. д. и радиальных изменений давления в паровой фазе оказывается пренебрежимо малым. Нестационарность возникает исключительно из-за значительных тепловых эффектов внутри капли и связанных с ними изменений в движущих силах со стороны пара.